Nanomed. J. 9(1): 57-10, Winter 2022

RESEARCH PAPER

Evaluation of the anti-melanogenic activity of nanostructured lipid carriers containing auraptene: A natural anti-oxidant agent

Sara Daneshmand [1], RezvanYazdian-Robati [2] , Mahmoud Reza Jaafari [3, 4], Jebrail Movaffagh [5, 6], Bizhan Malaekeh-Nikouei [3], Mehrdad Iranshahi [7], Shiva Golmohammadzadeh [3, 6]*, Zahra Tayarani-Najaran [7, 8]*

[1]Department of Pharmaceutics, School of Pharmacy, Zabol University of Medical Sciences, Zabol, Iran
[2]Molecular and Cell Biology Research Center, Faculty of Medicine, Mazandaran University of Medical Sciences, Sari, Iran
[3]Nanotechnology Research Center, Pharmaceutical Technology Institute, Mashhad University of Medical Sciences, Mashhad, Iran
[4]Department of Pharmaceutical Nanotechnology, School of Pharmacy, Mashhad University of Medical Sciences, Mashhad, Iran
[5]Targeted Drug Delivery Research Center, Pharmaceutical Technology Institute, Mashhad University of Medical Sciences, Mashhad, Iran
[6]Department of Pharmaceutics, School of Pharmacy, Mashhad University of Medical Sciences, Mashhad, Iran
[7]Biotechnology Research Center, Pharmaceutical Technology Institute, Mashhad University of Medical Sciences, Mashhad, Iran
[8]Department of Pharmacodynamics and Toxicology, School of Pharmacy, Mashhad University of Medical Sciences, Mashhad, Iran

ABSTRACT

Objective(s): In this work, we loaded Auraptene (AUR) into nanostructured lipid carriers (NLCs) and performed an assessment on inhibitory activities of the obtained AUR-NLCs on melanogenesis.

Materials and Methods: AUR-NLCs were prepared through a high shear homogenization and ultrasound method.

Results: Entrapment efficiency and Particle size of the optimized formulation were 103.1±4.9 nm and 89.56±3.75. The TEM outcomes exhibited the spherical shape of our nanoparticles, while the DSC analysis revealed the lack of any drug-lipid incompatibility throughout the formulations. A prolonged drug-release was observed from AUR-NLCs when compared to the AUR-solution. According to results, this product can significantly attenuated the activity of cellular tyrosinase and ROS content with minimal cytotoxic effects in B16F10 cell line, which in contrast to AUR-solution. Moreover, the western blotting analysis was indicative of AUR-NLCs ability to inhibit melanogenesis through the suppression of MITF and act much more efficiently than AUR-solution.

Conclusion: AUR-NLCs can offer merits as a natural anti-tyrosinase agent for the treatment of hyperpigmentory disorders.

Keywords: Anti-tyrosinase; Auraptene; Melanin; Melanogenesis; NLC

How to cite this article

Daneshmand S, Yazdian-Robati R, Jaafari MR, Movaffagh J, Malaekeh-Nikouei B, Iranshahi M, Golmohammadzadeh Sh, Tayarani Najaran Z. Evaluation of the anti-melanogenic activity of nanostructured lipid carriers containing auraptene: A natural anti-oxidant agent. Nanomed J. 2021; 9(1): 57-66. DOI: 10.22038/NMJ.2021.62354.1645

INTRODUCTION

Although the fabrication of melanin in melanocytes has a proficient role in the protection of skin, however, the overproduction of this material results in one of the most common skin problems known as hyperpigmentation. Tyrosinase is recognized as the principal imperative factor since it controls the production of melanin and therefore, its inhibition stands as an appealing strategy for the treatment of hyperpigmentation. Tyrosinase controls the rate-limiting steps of melanogenesis and converts tyrosine into dopaquinone to result in producing eumelanin

* *Corresponding Author Email: tayaraninz@mums.ac.ir; golmohamadzadehsh@mums.ac.ir*

Note. This manuscript was submitted on October 10, 2020; approved on January 10, 2021

and pheomelanin. Kojic acid and hydroquinone are exerted as conventional tyrosinase inhibitors in cosmetic formulations. However, their usage in skin disorders is quiet limited due to containing a low stability in formulations and poor skin permeation [1]. For this reason, researchers felt the necessity for the development of new tyrosinase inhibitors with low toxicity and more efficiency. In this regard, auraptene (AUR) has been previously introduced as an efficient anti-tyrosinase agent with minimal cytotoxicity on B16F10 melanoma cells next to inhibiting tyrosinase activity [2]. However, AUR's delivery through the stratum corneum (SC) is low due to its poor water solubility. Consequently, the application of permeation enhancers or frequent administration are necessary to enhance the efficiency of this product, which may irritate the skin or decrease the patients' compliance. In addition, the direct contact of chemical substances with SC might increase the chances of dermal toxicity [3]. To avoid direct skin contact, new delivery systems attempted to encapsulate the drug and increase the efficiency of drug penetration into the skin. In this regard, nanostructured lipid carriers (NLCs) attracted the focus of many as a profitable skin delivery system that can optimize the conventional delivery systems while being formulated with biocompatible lipids and safe surfactants. Forming an occlusive film by NLCs helps to decrease the water loss and consequently detach the cell contacts in SC to finally increase the rate of drug penetration [4].

Hence, the development of AUR-NLCs can be beneficial for the treatment of hyperpigmentation since it leads to increasing the cell penetration and tyrosinase inhibition activity of AUR [5]. In this study, we considered the application of AUR-NLC as an efficient delivery system to optimize the penetration of AUR and decrease its direct toxicity as an anti-tyrosinase agent. AUR was encapsulated in lipid nanoparticles based on perecirol and glycerol mono stearate. NLCs were optimized and characterized by different parameters, while their melanogenesis inhibition activities were determined through the performance of various assays that provide measurements on melanin content, ROS, tyrosinase activity and the level of intra cellular tyrosinase, and MITF. In addition, we evaluated the toxicity profile of AUR-loaded NLCs (AUR-NLCs) in B16F10 melanoma cells.

MATERIALS AND METHODS

Materials

Glycerol monostearate (GMS) and glycerylpalmitostearate (Precirol ATO5), were kindly gifted from Gattefossé (France). Poloxamer 188 (Uniqema, Belgium), span 80, Resazurin, 2',7'-dichlorofluorescein diacetate (DCF-DA), H_{2O2} and RPMI 1640 were purchased from Sigma-Aldrich; ECL western blotting detection reagent and a western blot apparatus set from Bio-RaD; Antibodies from Cell Signaling Technology (USA); APS, dimethylsulfoxide (DMSO), and tetramethylethylenediamine (TEMED) from Merck; penicillin/streptomycin 100 X and fetal bovine serum (FBS) from Gibco. Analytical grade of solvents and chemicals from Dr. Mojallali Chemical Complex Co. Auraptene (7-geranyloxycoumarin) was purchased from the Golexir Pars Co. (purity ≥ 95%).

Methods

Experimental design

Design expert software (Version DX7Trial) was utilized for the optimization of Particle size, PDI, and zeta potential (Z-P). In addition, central composite design was used (three responses and five factors) for statistical analyses and optimization. Particle size (nm), Z-P, and PDI were selected as the response variables, while drug concentration (X1), surfactant concentration (X2), feed ratio of surfactant (poloxamer188/span80) (X3), feed ratio of solid lipid /liquid lipid (X4), and feed ratio of solid lipid (% GMS/total lipid) (X5) represented independent parameters [6-8].

Preparation of NLCs

Prercirol and GMS were selected and used for the preparation of AUR-NLCs. In addition, span 80 and poloxamer were applied as surfactants due to their biocompatibility and low toxicity. The fabrication of AUR-loaded NLC was completed through a hot high-pressure homogenization technique [9]. Ultra-Turrax T25 (IKA T10, Germany) was utilized for the homogenization of hot lipid phase (lipids, span 80 and AUR) throughout the water phase (Poloxamer 188) for 5 min at 11500 rpm. Furthermore, a probe sonicator (Bransonic, USA) was exerted to sonicate the dispersion with the power delivery of 100% and 70s on/30s off cycles for 3 min; the formulations were cooled down to room temperature [10].

Particle size, polydispersity index (PDI), and zeta potential measurement

The measurements of zeta potential, mean particle size, and PDI were determined by the means

of Dynamic light scattering (ZetaSizer Nano-ZS; Malvern Instruments Ltd., United Kingdom). All of the experiments were conducted in triplicate [11].

Determination of the encapsulation efficiency of AUR in NLCs

The amount of entrapped AUR within the NLCs was measured through the application of direct method, which was performed in accordance with the description of our previous study. In brief, the separation of free crystals of AUR in formulation was carried out through filtration by a nitrocellulose membrane (Millipore). 100 µl of the filtrate was diluted with 900 µl of methanol/ chloroform (2:1) and vortexed for 30 sec. Then, quantification was performed with high-performance liquid chromatography (HPLC). We exerted similar analytical Knauer HPLC system and conditions to that of our previous study. The standard calibration curve of AUR (5-50 µg/ml) was observed to be linear (r2=0.9980), while the EE percentage was calculated as the following:

EE% = 100× (Auraptene after purification)/ (Total initial drug content) Eq. (1)

There was a possibility that the some concentration of drug remained separated and the filtering step was required to obtain the actual entrapped drug in order to eliminate the risk of measuring a false high rate of drug encapsulation. In the current study, the formulations were filtered to assuredly prevent the passage of detached drug through the filter and only gather the drug containing nanoparticles [3, 12].

Morphological studies

The morphology of AUR-NLCs observed by the utilization of transmission electron microscopy (CEM 902A; Zeiss, Germany). For this purpose, the formulation was placed on copper grids and stained with 0.2% (w/v %) uranyl acetate [13, 14].

Differential scanning calorimetry (DSC) analysis

In regards to recrystallization index, the DSC procedure was performed by the usage of Mettler DSC 821e (Mettler Toledo, Gießen, Germany) to evaluate the thermal analysis of AUR, drug-free NLC, and AUR-loaded NLC formulations. DSC is utilized to assess the possibility of excipient-drug interactions and the melting point of formulation. The samples were weighed in an aluminum pan and scanned at 25-200°C. Considering the heating rate of 5˚C/min, the obtained DSC curves were applied to investigate drug-excipient interactions [15].

Release study

To complete the release study, the abdominal skins of mice (BALB/c) were shaved and excited to be soaked in normal saline for 2 h for removing their subcutaneous fat. The study was done on a Franz diffusion cell with a diffusion area of 4.54 cm^2 with SC facing the donor compartment· The receptor cell was filled up with 20 ml of PBS and SLS 1% to be maintained at 37 ◦C by being stirred at 200 rpm. Formulations of 0.5% AUR-solution and 0.5% AUR-loaded NLC were applied to the skin surface. A one mL sample of the receptor was discharged at 1, 2, 3, 4, 6, 8, and 24 h and the same volume of fresh PBS was added to the receptor compartment. As the last step, we exerted an HPLC method to assay the samples [3].

Toxicity assessment of AUR-NLCs on melanoma cell line

B16F10 melanoma cell line (Cat. No C540) was purchased from the Pasteur Institute of Iran (Tehran, Iran) and stored in a humidified atmosphere (90%) that contained 5% CO2 at 37°C. Cells were cultured in RPMI-1640 (Bioidea, Iran) with 10% (v/v) fetal bovine serum, 100 U/ mL of penicillin, and 100 µg/mL of streptomycin. Thereafter, we performed rezasurin assay to discover the non-cytotoxic concentration of AUR-Solution and AUR-NLCs on cells. Once 2×104 Cells per well were seeded in a 96-well plate, they were exposed to different concentrations of AUR-Solution and AUR-NLCs (2-500 µg/mL) for 24 h [16].

Determination of cellular tyrosinase activity in melanoma cells

The ability of B16F10 cells to oxidize L-3,4-dihydroxyphenylalanine (L-DOPA) was characterized as an index for tyrosinase activity. Briefly, 5×10^4 B16F10 cells per each well of 24-well plate were incubated with AUR-NLCs and AUR-Solution at 1-250 µg/mL for 24 h. Then, cell lysate lysed in the PBS that contained 1% Triton X-100 was mixed with 2 mL of L-DOPA (2 mg/mL). After 2 h of incubation at 37°C, the absorbance was read at 475 nm by the application of a micro-plate reader (BioTek, USA) [17].

Determination of cellular ROS levels

2×10^4 B16F10 cells were seeded in 96-well plates overnight to be treated with AUR-NLCs afterwards at concentrations of 125, 250 µg/mL for 24 h. In the following, H_2O_2 (24 mM) was added for the duration of 30 min and the obtained fluorescence intensity between the samples was compared by the usage of dichloro-dihydro-fluorescein diacetate (DCFH-DA). DCFH-DA was excited at 485 nm and the emission was read at 528 nm through a Synergy H4 microplate reader (BioTek, USA) [18].

Determination of melanin content of melanoma cells

5×10^4 B16F10 cells were treated with different concentrations (125 and 250 µM) of AUR-NLCs, which were homogenized in the 2 M solution of sodium hydroxide (100 µL) for 30 min at 100 °C. The absorptions of melanin for each sample was compared with the control at 405 nm [19].

Western blotting

50 µg Protein lysate of 106 B16F10 melanoma cells were treated with 125 and 250 µM of AUR-NLCs for 24 h to be separated afterwards according to molecular weight by the usage of 10% SDS-polyacrylamide gel electrophoresis. In the following, we transferred the samples to polyvinylidene difluoride membranes to perform the process of block in 5% skim milk in TBST buffer at 4°C. Each membrane was washed three times in TBST buffer and incubated with a primary antibody, which included rabbit anti-tyrosinase antibody (1:300) and anti-MITF antibody (1:300), as described in the related protocol. Afterwards, the anti-rabbit IgG (1:2000) was appended as the secondary antibody and the bands were detected by the means of ECL Prime Western Blotting Detection System (BioRaD, USA). Furthermore, we quantified the band intensities by using Quantity One software (Bio-Rad) to measure the optical densities [16, 20].

Statistical analysis

All of the experiments were carried out in triplicate and the obtained results were presented as mean ± standard deviation (SD). The analysis of variance followed by Dunnett tests was performed through the application of GraphPad Prism 5.0 software. $P<0.05$ was considered statistically significant difference between samples [21].

RESULTS AND DISCUSSION

Optimization of NLCs

The optimization of every 26 experimental runs was executed by the usage of CCD (Central Composite Design) (Table 1). Considering the analysis results, the formulation with appropriate PDI, Z-P, and particle size was chosen for being applied throughout the in vitro evaluations. The obtained outcomes indicated that the optimized NLCs with high Z-P, low PDI, and proper mean particle size was consisted of an AUR (drug) concentration of 0.5%, a feed ratio of solid lipid to liquid lipid of 3%, lipid ratio of 30%, surfactant concentration of 1.5%, and surfactant ratio of 2. The mathematical predicted model of NLCs was prepared three times to validate the predicted formulation. The accuracy of our experimental design was confirmed by the close similarity of experimental data to the predicted theoretical values. In conformity to Table 1, the observed values of three batches of NLCs were very close to the predicted values. The low percentage of bias indicated that the optimized formulation was reasonable.

Particle size, PDI, and zeta potential measurement

The particle size, PDI, and zeta potential of all the formulations are presented in Table 2, whereas the optimized formulation of AUR-NLC was reported from run 2. Our study data displayed that the mean particle size of NLCs was 103.1 nm.

Table 1. Comparison between predicted and experimental values in the NLCs prepared under predicted optimum conditions

Response	Experimental values	Predicted values	% Bias *
Size (nm)	103.1±3.43	99.96	3.14
z-p (mV)	-21.2±4.65	-21.4	0.9
PDI	0.29±0.037	0.28	3.5

*%Bias: (predicted value - experimental value)/predicted value * 100

Table 2. Obtained responses and experimental runs for different formulations of AUR-NLCS

Run	X_1:Auraptene w/w%	X_2:surfactant w/w%	[a]X_3:Feed ratioe of surfactant%	X_4: feed ratio of solid lipid to liquid lipid	[b]X_5:feed ratioe of solid lipid%	Z-average size (nm)±SD	Zeta potential (mV)±SD	Polydispersity±SD
1	0.50	2.50	3.00	4.00	20.00	200±5.2	-22.5±2.5	0.3±0.04
2	0.50	1.50	2.00	3.00	30.00	103.1±4.9	-21.2±1.2	0.29±0.06
3	1.75	1.50	2.00	3.00	30.00	254.6±8.5	-24±3.1	0.302±0.09
4	3.00	2.50	3.00	2.00	20.00	110.7±6.3	-20.3±1.9	0.236±0.12
5	1.75	1.50	2.00	3.00	30.00	347±8.4	-24.6±2.4	0.310±0.04
6	3.00	0.50	1.00	4.00	40.00	301.2±3.6	-22.7±1.4	0.3±0.06
7	1.75	1.50	2.00	3.00	30.00	330±9.3	-20.7±0.5	0.372±0.11
8	1.75	0.50	2.00	3.00	30.00	317.4±10.1	-20.8±2.1	0.351±0.09
9	3.00	2.50	1.00	4.00	20.00	324±4.8	-21.9±1.8	0.387±0.05
10	3.00	0.50	3.00	2.00	40.00	267.7±2.7	-22.1±1.3	0.298±0.15
11	1.75	1.50	2.00	3.00	30.00	389.5±9.1	-22±2.5	0.311±0.09
12	1.75	1.50	2.00	3.00	40.00	408.3±11.9	-20.1±1.3	0.44±0.04
13	3.00	1.50	2.00	3.00	30.00	415.3±10.4	-29.1±1.9	0.471±0.18
14	0.50	0.50	3.00	4.00	40.00	318.5±5.6	-19.4±2.7	0.301±0.13
15	0.50	0.50	1.00	2.00	20.00	108.4±3.9	-23±2.6	0.21±0.03
16	1.75	1.50	3.00	3.00	30.00	339.6±3.1	-23.7±1.3	0.348±0.07
17	3.00	0.50	3.00	4.00	20.00	300±7.4	-21.7±1.8	0.311±0.06
18	1.75	1.50	2.00	4.00	30.00	406.3±8.6	-21.6±3.1	0.3±0.12
19	0.50	2.50	1.00	4.00	40.00	263.1±5.7	-22.3±2.9	0.452±0.13
20	1.75	1.50	2.00	3.00	20.00	290.5±6.4	-21.9±2.4	0.268±0.21
21	1.75	1.50	1.00	3.00	30.00	376.1±3.9	-21.9±1.3	0.307±0.05
22	3.00	2.50	1.00	2.00	40.00	254.1±5.3	-21.4±1.7	0.309±0.21
23	1.75	1.50	2.00	2.00	30.00	160.6±5.1	-19.4±1.5	0.215±0.11
24	0.50	2.50	3.00	2.00	40.00	140.9±3.8	-21.1±2.3	0.264±0.08
25	1.75	2.50	2.00	3.00	30.00	304.2±7.5	-22.4±2.6	0.304±0.02
26	1.75	1.50	2.00	3.00	30.00	303.4±4.8	-23.9±2.1	0.315±0.03

[a] Feed ratio of surfactant%: poloxamer188/Span80.
[b] Feed ratio of lipid%: % Glycerol Monostearate/total lipid

According to the other reports, the small size of NLCs is one of its main properties considering how the particle size<200 nm can enhance skin penetration and improve occlusive qualities of the drug [22]. High values of zeta potential decreases the aggregation of nanoparticles and consequently increases the physical stability of disperse systems. In this investigation, the zeta potential of optimal formulation was obtained to be -21.2 mV. In addition, the application of poloxamer 188 as a surfactant provides a higher sterical stabilization for the nano carriers and therefore, we achieved a suitable physical stability in our study formulation [23].

Entrapment efficiency (EE)

In this section, we measured the EE % of optimized formulation to be 89.56±3.75. The factors of disordered structure of two kinds of lipid and the high lipophilicity of AUR are the reasons behind the increased percentage of EE. As a result, the low amount of free crystals of AUR is prevented from having contact with the skin which reduces the rate of irritation [11].

Morphology of AUR-loaded NLCs

Transmission electron microscopy was applied to observe the morphology of AUR-loaded NLCs.

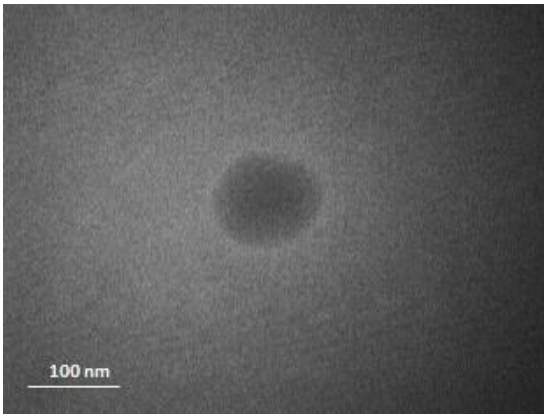

Fig 1. Transmission electron microscopy of AUR-loaded NLCs

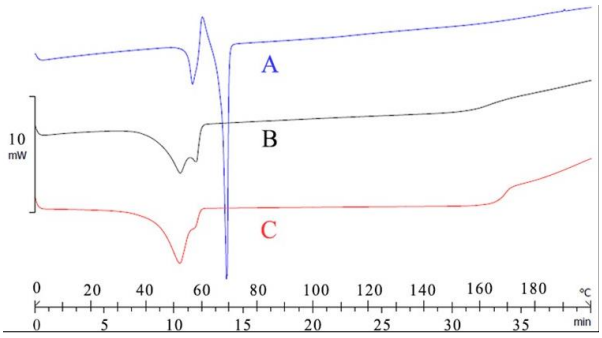

Fig. 2. DSC images of: (A) auraptene; (B) auraptene-loaded nanostructured lipid carriers; and (C) Drug-free nanostructured lipid carriers

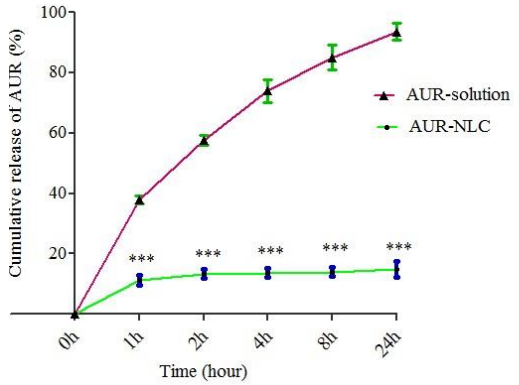

Fig. 3. Drug release in AUR-solution and AUR-NLCs over the 24 h period (n = 3, Mean±SD).. *** P<0.001 compared to AUR-solution

Next to the demonstrated spherical shape of nanoparticles, Fig. 1 displays the size of most of the nanoparticles to be close to 100 nm, which is similar to the data represented by zeta-sizer of Malvern in Table 1. Compared to the other shapes of nanoparticles, the spherical shape of particles is indicative of the lowest contact surface with aqueous phase and the longest route to release. Additionally, spherical particles can provide higher drug stability as well as controlled-release [24].

Differential scanning calorimetry (DSC) analysis

DSC is an appropriate method to investigate the crystalline nature of substances. Fig. 2 presents the DSC curves of AUR-loaded nanocarriers, drug-free NLCs, and pure AUR. The melting point of AUR recorded at 70◦C demonstrates the crystalline nature of this substance as a coumarin. Moreover, DSC data can reveal whether a drug is incorporated into the particles matrix. The absence of melting peak for crystalline AUR throughout the thermogram of AUR-NLCs determines the adopted amorphous state of AUR in the NLCs matrix [25].

Drug release

In vitro release study was carried out to distinguish the drug-release behavior of nanoparticles. In this regard, we assessed the release of AUR from the NLCs for 24 h and observed the controlled-release property. According to the results, 14.85% of the drug was released from AUR- NLC, while 93.60% was released from the AUR-solution in 24 h. The drug diffusion in AUR-solution was higher than that of AUR-NLCs (P<0.001; Fig. 3). Furthermore, the outcomes were suggestive of a biphasic release

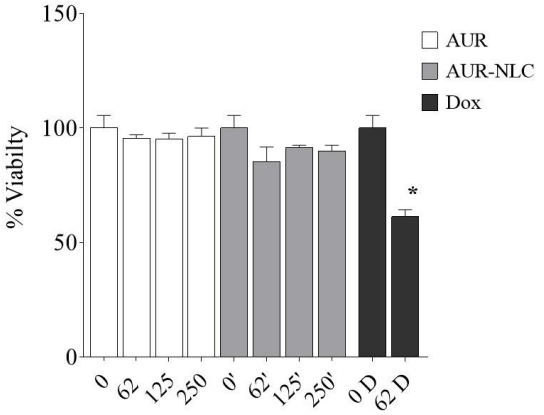

Fig. 4. Effect of different concentrations of AUR-Solution and AUR-NLCs on cell viability (n=3, Mean±SD).· *** P<0.001 compared to control

for AUR-NLCs formulations. Considering the burst release of AUR from AUR-NLCs in the first 30 min, it should be noted that an initial fast release provides a high concentration that enhances skin penetration, while the sustained release of AUR over 24 h improved the prolonged release and biologic effects of AUR[26].

Effect of different concentration of AUR-NLCs on cell survival

In this study, resazurin assay was performed in order to monitor cell viability, for which the B16F10 cells were treated with different concentrations of AUR-Solution and AUR-NLCs. In conformity to Fig. 4, the treatment of cells with 0-250 µM of AUR-Solution and AUR-NLCs did not result in any significant cytotoxic effects. Based on the resazurin

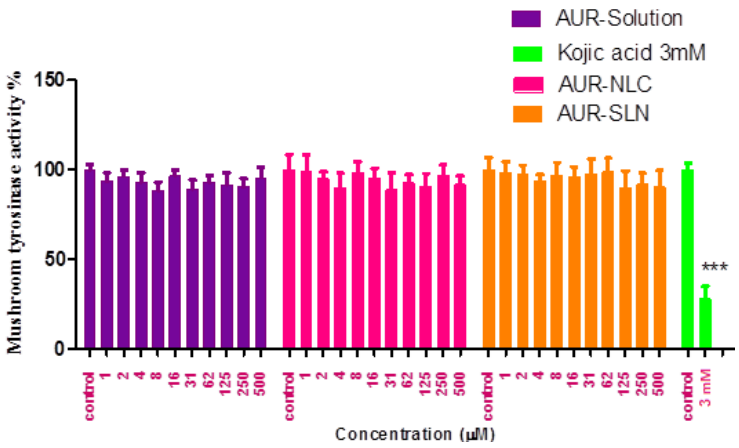

Fig. 5. Effect of different concentrations of AUR-Solution and AUR-NLCs on mushroom tyrosinase activity

assay, more than 90% of the cells remained viable after exposure to AUR and AUR-NLCs even at the highest concentration (250 µM) for 48 h (Fig. 4). These results confirmed that the anti-melanogenic activity of AUR and AUR-NLCs in B16F10 murine melanoma cells was not associated with cytotoxic effects.

Effect of different concentration of AUR-Solution and AUR-NLCs on tyrosinase activity

Tyrosinase is a key enzyme in the first step of melanin production, which is consequently involved in hyperpigmentation as well and therefore, the inhibition of this substance is considers as a dominant approach in the development of new whitening agents [27]. To evaluate the mechanism of inhibitory effect on tyrosinase activity, we investigated the impact of AUR-Solution and AUR-NLCs on both mushroom and cellular tyrosinase in B16F10 melanoma cells. Both of the compounds were incapable of causing any effects on mushroom tyrosinase activity (Fig. 5), however, the results were indicative of the significance inhibition of AUR-NLCs at 125 and 250 µM in regards to cellular tyrosinase activity.

Effect of different concentration of AUR-Solution and AUR-NLCs on cellular tyrosinase

The effects of AUR and AUR-NLCs on the catalytic activities of cellular tyrosinase are illustrated in Fig. 6. Apparently, penetrating into cells is an essential step for anti-tyrosinase activity and AUR-NLCs can improve the accessibility of AUR to cells.

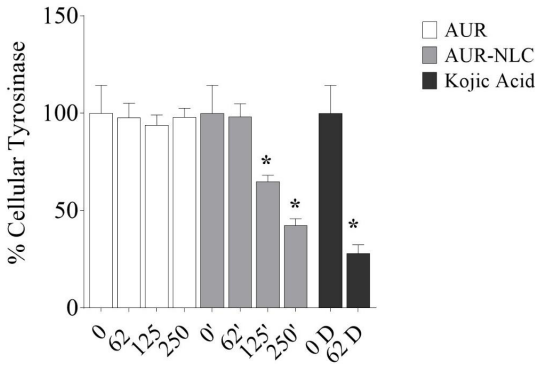

Fig. 6. Effect of different concentration of AUR-Solution and AUR-NLCs on cellular tyrosinase activity in B16F10 murine melanoma cells. (n=3, Mean±SD). · *** P< 0.001 compared to control

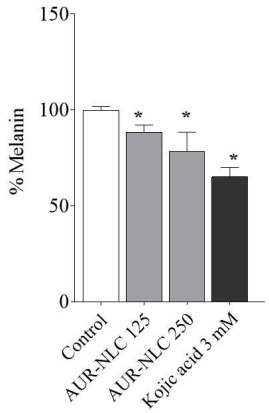

Fig. 7. Effect of different concentration of AUR-NLCs on melanin content in B16F10 murine melanoma cells. (n=3, Mean±SD). ** P< 0.01, as compared to control

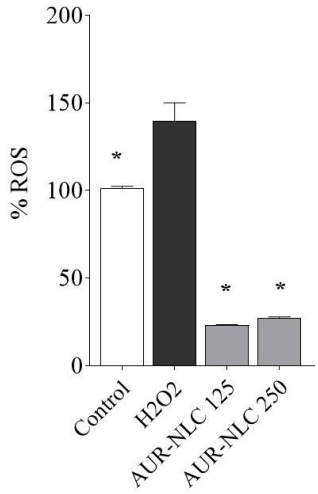

Fig. 8. Anti-oxidant effects of different concentration of AUR-NLCs on cellular reactive oxygen species (ROS) levels in B16F10 murine melanoma cells. (n = 3, Mean±SD). *** P<0.001 compared to control

Effect of different concentration of AUR-NLCs on the synthesis of melanin

We performed an assessment on the inhibitory effect of different concentrations of AUR-NLCs on melanin content of B16F10 cells to determine their anti-melanogenic activity. The inhibitory effects of AUR-NLCs (125 and 250 µM) reflected the reduced amount of melanin synthesis when compared to the control (kojic acid) and AUR (Fig. 7). The production of melanin is the final step of melanogenesis. A decrease in the amount of melanin indicates the inhibitory effect of AUR-NLC on tyrosinase, which eventually leads to a reduction in the melanin content of cells.

Effect of concentration of AUR-NLCs on cellular ROS level

The intracellular ROS levels were determined to measure the anti-oxidant capacity of AUR in cells that were treated with 24 mM of H_2O_2 alone or 125 and 250 µM of AUR-NLCs in B16F10 melanoma cells. As it is displayed in Fig. 6, the pretreated cells with AUR-NLCs were able to significantly suppress the induced oxidative stress by H_2O_2 (Fig. 8). According to the gathered data, the anti-tyrosinase activity of natural compounds in general and citrus crude extracts are greatly linked to the anti-oxidant activity [28, 29]. Therefore, it is assumable that both of the cellular tyrosinase inhibition and ROS scavenging activity participate in the anti-melanogenic activity of auraptene.

Western blotting analysis of the amount of tyrosinase and MITF in AUR-NLCs-treated cells

The complex cascade of enzymes, including tyrosinase, TRP-1, TRP-2, and MITF (Microphthalmia-associated transcription factor), were applied to modulate the development of melanocyte by regulating various differentiations and cell-cycle progression genes [18]. In order to understand the precise molecular mechanisms that underly the reduction of melanogenesis by AUR-NLCs, we measured the amount of MITF and tyrosinase by the usage of western blot assay [16]. According to Fig. 9, AUR-NLCs were abled to significantly reduce the protein levels of MITF in a dose-dependent manner. Our results suggest that the melanogenesis inhibition by AUR-NLCs occurs through the down-regulation of MITF and its downstream target gene, which mainly includes tyrosinase.

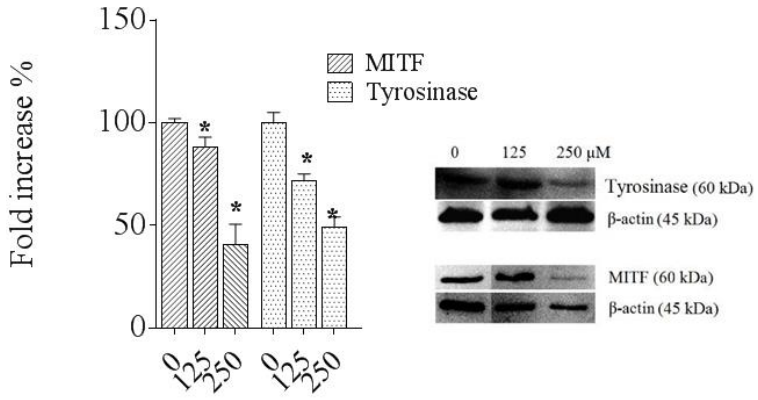

Fig. 9. Effect of the AUR-NLCs on the amount of tyrosinase, and MITF Protein in B16F10 melanoma cells. (n = 3, Mean±SD). · *** P< 0.05, and · *** P< 0.001 compared to β-actin

In conclusion, AUR-NLCs can be nominated as an applicable whitening agent due to its ROS-scavenging and anti-tyrosinase properties. The application of colloidal nano-carriers improve the obtained bioavailability, cell penetration, and drug movement throughout the cells. In this work, we exerted NLCs to encapsulate AUR and enhance the compounds efficacy as an anti-oxidant and anti-melanogenic agent. There are strong evidences on the impacts of using nano-carriers with a size below 200 nm on improving cell penetration and movement in cytosol [30].

Further evidences confirmed the achievement of long-term retention of drug in the skin through the utilization of nano lipid carriers [31]. Similarly, our previous study reported parallel results when the lipid nano-carriers were compared to non-encapsulated AUR [3]. Therefore, the effective inhibition of cellular tyrosinase is expected upon the topical usage of AUR-NLCs on skin. Altogether, the finding of present study can stand as convincing evidences for the application of AUR-NLCs as a whitening agent throughout skin lightening formulations. AUR-NLC can be a suitable nano lipid carrier through the treatments of hyperpigmentary disorders due to the multiple properties of NLCs, which include being biodegradable, providing an slow and sustained release, and offering protection for the drugs [32].

CONCLUSION

In the current study, AUR was successfully loaded in NLCs with a sufficient encapsulation efficiency. In vitro studies revealed the acceptable release and skin-permeation of AUR from the NLCs matrixes. According to in vitro cellular evaluations, AUR-NLCs can effectively prevent melanogenesis with minimal cytotoxicity and therefore, this suitable system can be recommended to be applied throughout the treatment of skin hyperpigmentation.

ACKNOWLEDGMENTS

This work was supported by Grant number 930379 from Research Affairs of Mashhad University of Medical Sciences. The authors are thankful to Gattefossé (France) for providing the gift samples.

CONFLICT OF INTEREST

The authors report no Conflict of interest in this work.

REFERENCES

1. Rigon RB, Fachinetti N, Severino P, Santana MH, Chorilli M. Skin delivery and in vitro biological evaluation of trans-resveratrol-loaded solid lipid nanoparticles for skin disorder therapies. Molecules. 2016; 21(1): 116.
2. Kim M-J, Kim SS, Park K-J, An HJ, Choi YH, Lee NH, et al. Anti-melanogenic Activity of Auraptene via ERK-mediated MITF Downregulation. Cosmetics. 2017; 4(3): 34.
3. Daneshmand S, Jaafari MR, Movaffagh J, Malaekeh-Nikouei B, Iranshahi M, Moghaddam AS, et al. Preparation, characterization, and optimization of auraptene-loaded solid lipid nanoparticles as a natural anti-inflammatory agent: *In vivo* and *in vitro* evaluations. Colloids Surf B. 2018.
4. Das S, Ng WK, Tan RB. Are nanostructured lipid carriers (NLCs) better than solid lipid nanoparticles (SLNs): development, characterizations and comparative evaluations of clotrimazole-loaded SLNs and NLCs? Eur J Pharm Sci. 2012; 47(1): 139-151.
5. Al-Amin M, Cao J, Naeem M, Banna H, Kim M-S, Jung Y, et al. Increased therapeutic efficacy of a newly synthesized tyrosinase inhibitor by solid lipid nanoparticles in the topical treatment of hyperpigmentation. Drug Des Devel Ther. 2016; 10: 3947.
6. Kamali H, Khodaverdi E, Hadizadeh F, Ghaziaskar S. Optimization of phenolic and flavonoid content and antioxidants capacity of pressurized liquid extraction from Dracocephalum kotschyi via circumscribed central composite.J Supercrit Fluids. 2016; 107: 307-314.
7. Daneshvar M, Kamali H, Masoomi M, Ghaziaskar H. Supercritical carbon dioxide grafting of glycidyl methacrylate onto medium density polyethylene and purification of residual monomer and initiator. J Supercrit Fluids. 2012; 70: 119-125.
8. Amiri N, Moradi A, Tabasi SAS, Movaffagh J. Modeling and process optimization of electrospinning of chitosan-collagen nanofiber by response surface methodology. Mater Res Express. 2018; 5(4): 045404
9. Müller RH, Rühl D, Runge S, Schulze-Forster K, Mehnert W. Cytotoxicity of solid lipid nanoparticles as a function of the lipid matrix and the surfactant. Pharm Res. 1997; 14(4): 458-462.
10. Pardeike J, Schwabe K, Müller RH. Influence of nanostructured lipid carriers (NLC) on the physical properties of the Cutanova Nanorepair Q10 cream and the *in vivo* skin hydration effect. Int J Pharm. 2010; 396(1-2): 166-173.
11. Okonogi S, Riangjanapatee P. Physicochemical characterization of lycopene-loaded nanostructured lipid carrier formulations for topical administration. Int J Pharm. 2015; 478(2): 726-735.
12. Daneshmand S, Golmohammadzadeh S, Jaafari MR, Movaffagh J, Rezaee M, Sahebkar A, et al. Encapsulation challenges, the substantial issue in solid lipid nanoparticles characterization. J Cell Biochem. 2018; 119(6): 4251-4264.
13. Han S, Kwon S, Jeong Y, Yu E, Park S. Physical characterization and in vitro skin permeation of solid lipid nanoparticles for transdermal delivery of quercetin. Int J Cosmet Sci. 2014; 36(6): 588-597.
14. Yang S, Zhu J, Lu Y, Liang B, Yang C. Body distribution of camptothecin solid lipid nanoparticles after oral administration. Pharm Res. 1999;16(5):751-757.
15. Araujo J, Gonzalez-Mira E, Egea M, Garcia M, Souto E. Optimization and physicochemical characterization of a triamcinolone acetonide-loaded NLC for ocular antiangiogenic applications. Int J Pharm. 2010; 393(1-2): 168-176.

16. Hashemi-Shahri SH, Golshan A, Mohajeri SA, Baharara J, Amini E, Salek F, et al. ROS-scavenging and anti-tyrosinase properties of crocetin on B16F10 murine melanoma cells. Curr Med Chem Anticancer Agents. 2018; 18(7): 1064-1069.
17. Emami SA, Yazdian-Robati R, Sadeghi M, Baharara J, Amini E, Salek F, et al. Inhibitory effects of different fractions of Nepeta satureioides on melanin synthesis through reducing oxidative stress. Res Pharm Sci. 2017; 12(2): 160.
18. Qiao Z, Koizumi Y, Zhang M, Natsui M, Flores MJ, Gao L, et al. Anti-melanogenesis effect of Glechoma hederacea L. extract on B16 murine melanoma cells. Bioscience, biotechnology, and biochemistry. 2012; 76(10): 1877-1883.
19. Kamagaju L, Morandini R, Bizuru E, Nyetera P, Nduwayezu JB, Stévigny C, et al. Tyrosinase modulation by five Rwandese herbal medicines traditionally used for skin treatment. J Ethnopharmacol. 2013; 146(3): 824-834.
20. Hassani FV, Abnous K, Mehri S, Jafarian A, Birner-Gruenberger R, Robati RY, et al. Proteomics and phosphoproteomics analysis of liver in male rats exposed to bisphenol A: Mechanism of hepatotoxicity and biomarker discovery. Food ChemToxicol. 2018; 112: 26-38.
21. Hassani FV, Mehri S, Abnous K, Birner-Gruenberger R, Hosseinzadeh H. Protective effect of crocin on BPA-induced liver toxicity in rats through inhibition of oxidative stress and downregulation of MAPK and MAPKAP signaling pathway and miRNA-122 expression. Food Chem. Toxicol. 2017; 107: 395-405.
22. Zhang W, Li X, Ye T, Chen F, Sun X, Kong J, et al. Design, characterization, and *in vitro* cellular inhibition and uptake of optimized genistein-loaded NLC for the prevention of posterior capsular opacification using response surface methodology. Int J Pharm. 2013; 454(1): 354-366.
23. Bikkad ML, Nathani AH, Mandlik SK, Shrotriya SN, Ranpise NS. Halobetasol propionate-loaded solid lipid nanoparticles (SLN) for skin targeting by topical delivery. J Liposome Res. 2014; 24(2): 113-123.
24. Mosallaei N, Jaafari MR, Hanafi-Bojd MY, Golmohammadzadeh S, Malaekeh-Nikouei B. Docetaxel-loaded solid lipid nanoparticles: Preparation, characterization, *in vitro*, and *in vivo* evaluations. J Pharm Sci. 2013; 102(6): 1994-2004.
25. Golmohammadzadeh S, Mortezania S, Jaafari MR. Improved photostability, reduced skin permeation and irritation of isotretinoin by solid lipid nanoparticles. Acta Pharm. 2012; 62(4): 547-562.
26. Kumar S, Bhanjana G, Kumar A, Taneja K, Dilbaghi N, Kim KH. Synthesis and optimization of ceftriaxone-loaded solid lipid nanocarriers. Chem Phys Lipids. 2016; 200: 126-132.
27. Chang T-S. Natural melanogenesis inhibitors acting through the down-regulation of tyrosinase activity. Materials. 2012; 5(9): 1661-1685.
28. Sarkar R, Arora P, Garg KV. Cosmeceuticals for hyperpigmentation: What is available? J Cutan Aesthet Surg. 2013; 6(1): 4-11
29. Solano F, Briganti S, Picardo M, Ghanem G. Hypopigmenting agents: an updated review on biological, chemical and clinical aspects. Pigment Cell Melanoma Res. 2006; 19(6): 550-571.
30. Teskač K, Kristl J. The evidence for solid lipid nanoparticles mediated cell uptake of resveratrol. Int J Pharm. 2010; 390(1): 61-69.
31. Limsuwan T, Boonme P, Khongkow P, Amnuaikit T. Ethosomes of Phenylethyl Resorcinol as Vesicular Delivery System for Skin Lightening Applications. Biomed Res Int. 2017; 2017.
32. Müller R, Petersen R, Hommoss A, Pardeike J. Nanostructured lipid carriers (NLC) in cosmetic dermal products. Adv Drug Deliv Rev. 2007; 59(6): 522-530.